Multi-Frequency Periodic Vibration Suppressing with FBLMS Algorithm in Active Magnetic Bearing-Rotor System

Jiang Kejian[1,a], Zhu Changsheng[1,b]
[1]College of Electrical Engineering, Zhejiang University, Hangzhou, 310027, China
[a]jkjofzju@163.com, [b]cszhu@hotmail.com

Abstract: In active magnetic bearing (AMB)-rotor system, a method for the multi-frequency periodic vibration suppressing is proposed by an adaptive structure with the finite-duration impulse response (FIR) filter. To cater for the requirement of the long duration impulse response filter arisen in the AMB-rotor system, the Fast Block Least Mean Square (FBLMS) algorithm is adopted to efficiently implement the computation of linear convolution and linear correlation at a computational cost far less than that of the conventional FIR filter of time domain. The unique feature of the FBLMS algorithm is characterized by no influence on the computational complexity, regardless of the number of the vibration frequency components within the range of sampling frequency. The convergence rate of each frequency component can be adjusted by assigning the individual step size parameter for each filter weight. Furthermore, each harmonic component of the vibration can be addressed respectively or together. The experimental results of the reciprocating simulating disturbance test and the rotating harmonic vibration test show that the proposed adaptive structure with the FBLMS algorithm can achieve the good effectiveness for suppressing the multi-frequency periodic vibration.

Keywords: AMB, Multi-Frequency Periodic Vibration, FBLMS, Fast Convolution, Fast Correlation, Overlap-Save

Introduction

In recent years, with the development of the active magnetic bearing (AMB) technology, more and more attentions have been attracted to the AMB application for its performance advantage. The AMB can not only provide the contactless supporting for the rotor, but also apply the real-time active electromagnetic force to suppress the rotor vibration. So far, there have been a great number of investigations into the use of magnetic bearings to control the rotor vibration. While most of these have aimed at reducing the rotor unbalance vibration which only contains a single frequency component[1-6], comparatively, a few have considered the rotor vibration with the more complex excitations [7-12]. For the practical rotor system, the multi-frequency periodic vibration is the most common vibration form, especially in the reciprocating and rotating machinery. The multi-frequency periodic vibration can be regard as the combination of a set of the multiple harmonic components or some individual simple harmonic (sinusoidal) components whose frequency is uncorrelated each other. In this study, the attention would be confined to the periodic vibration with multi-frequency in the AMB-rotor system.

Nonami et al.[6] achieved the unbalance vibration suppressing by the iterative algorithm which requires no knowledge about the dynamical property of the AMB system. Moreover, Nonami et al.[8] and Liu et al.[10] extended the algorithm of vibration suppressing from single frequency to multi-frequency. Nevertheless, their methods for multi-frequency[8,10] merely implements the same algorithm of single frequency in some multiple frequencies respectively. As a direct consequence, the computational complexity will sharply increase in direct proportion to the number of the frequencies considered. For a practical rotor system, the rotor vibration generally contains large numbers of the frequency components. At present, there is no hardware for signal processing has capability to deal with such great computational load in real time. Therefore, it is infeasible in the case that the vibration contains a great number of frequency components.

In this study, a method for the multi-frequency periodic vibration suppressing is proposed by an adaptive structure with the finite-duration impulse response (FIR) filter. To deal with the requirement for the adaptive filter with a long duration impulse response arisen in applications of the AMB rotor system, the Fast Block Least Mean Square (FBLMS) algorithm is adopted to efficiently implement the computation of linear convolution and linear correlation in order to considerably reduce the computational complexity. The unique feature of the FBLMS algorithm is no influence on the computational complexity, regardless of the number of the vibration frequency components within the range of sampling frequency, it would have. Moreover, the weights in the FBLMS algorithm have the intuitional relation with frequency. As a result, each harmonic component of the vibration can be addressed respectively or together.

1 Adaptive Vibration Suppressing in Time Domain

Considering the common control model of the AMB-rotor system as shown in Fig.1, $C(s)$, $A(s)$ and $R(s)$ are the transfer functions of the main control, the AMB and the rotor, respectively. Theoretically, any vibration disturbance can equivalently be regarded as the direct disturbance force acting on the rotor which denoted by $d(t)$. The rotor vibration response of $d(t)$ which denoted by $y_d(t)$ can directly be computed in the time domain by the convolution, whose discrete form shown as follows,

$$y_d(n) = \sum_{m=-\infty}^{\infty} d(m)h_R(n-m) = d(n) * h_R(n) \tag{1}$$

where $h_R(n)$ is the unit impulse response of the rotor system whose transfer function is $R(s)/1-C(s)A(s)R(s)$, and * is the symbol for discrete linear convolution.

In order to suppress the rotor vibration, an adaptive structure which consists of an adaptive filter and its weights adjustment algorithm is presented as showed in Fig. 1. $out(n)$ is the discrete control signal generated by the adaptive filter. Likewise, the rotor movement response of $out(n)$, which denoted by $y_{out}(t)$, can also be computed in the time domain by the convolution as follows:

$$y_{out}(n) = \sum_{m=-\infty}^{\infty} out(m)h_{AR}(n-m) = out(n) * h_{AR}(n) \tag{2}$$

where $h_{AR}(n)$ is the unit impulse response of the AMB system whose transfer function is $A(s)R(s)/1-C(s)A(s)R(s)$.

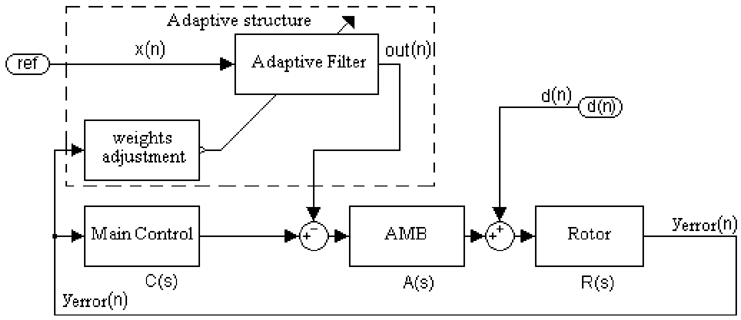

Fig.1 the control model of the AMB-rotor system with adaptive structure

The electromagnetic force generated by the AMB, combined with the disturbance force, leads to the dynamic movement of rotor. Considering $y_{out}(n)$ is a close match for $y_d(n)$, which means that it has the same magnitude and phase in each frequency component, the $y_d(n)$ would completely be counteracted by the response of the $y_{out}(n)$. If the $y_d(n)$ can not be counteracted by $y_{out}(n)$ exactly, the residual vibration induced by the control error can be detected in the rotor displacement signal, which is denoted by $y_{error}(n)$ as follows:

$$y_{error}(n) = y_0(n) + y_d(n) - y_{out}(n) = y_0(n) + d(n) * h_R(n) - out(n) * h_{AR}(n) \tag{3}$$

where $y_0(n)$ is the displacement signal without vibration disturbance.

According to the certain statistical criterion, which is also said to be the cost function, the adaptive algorithm adjusts the filter weights to minimize the error between $y_{out}(n)$ and $y_d(n)$ in a sense of the cost function. When $y_{out}(n) = y_d(n)$, the disturbance vibration will be eliminated. Among the cost functions, the Mean Square Error (MSE) is most popular and widely used in a variety of applications, because the MSE has the unique global minimum to lead to tractable mathematics. The MSE of the displacement signal is defined as

$$\mathrm{MSE} = \xi = E[| y_{error}(n) - 0 |^2] = E[| y_{error}(n) |^2] \tag{4}$$

where for convenience of discussion, the set value of rotor displacement is assumed to be zero. $E[\ ]$ denotes the statistical expectation operator. Because $y_{error}(n)$ contains the random noise component, the mean-value of $| y_{error}(n) |^2$ can only be computed by the statistical expectation operation.

When the finite-duration impulse response (FIR) filter is adopted as the adaptive filter in the adaptive structure, whose internal structure is shown in Fig.2, there are two theorems listed as follows to explain the theoretic feasibility for the multi-frequency periodic vibration suppressing. For the limit for the paper length, the proving procedure for these two theorems will be detailed in the long version of this paper.

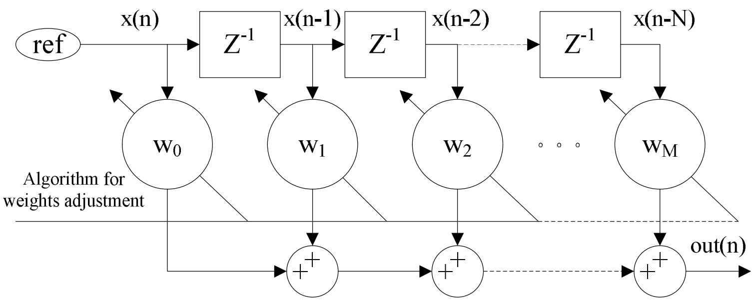

Fig.2 FIR adaptive filter structure

***Theorem** 1: In the case of steady disturbance, as long as the rotor displacement signal $y_{error}(n)$ is achieved the minimized MSE by adjusting the filter output signal $out(n)$ as shown in Fig.1, the y_{out} will be a close match for y_d as more as possible, namely, the rotor vibration is suppressed optimally.*

***Theorem** 2: In the case of steady disturbance, if the reference input signal which has correlation with the disturbance is known, it must be existent that a unique optimal solution W_{opt} of the FIR filter weights vector makes the filter to realize the MSE minimization of $y_d(n) - y_{out}(n)$.*

Because of the requirement for a priori statistics information about the processed data, the MSE is not suitable for the real-time computation. In practice application, the gradient vector of the MSE is generally estimated by the instantaneous value of gradient vector which can be solved by the iterative procedure. The resulting algorithm is widely known as the Least Mean Square (LMS) algorithm which is by far the most popular adaptive algorithm in practice. The essence of the LMS has been described in detail in [13,16-18].

2 Fast Block LMS Algorithm

2.1 Requirement of a Long Impulse Response

The aforementioned analysis only explains the theoretic feasibility for vibration suppressing by the adaptive structure shown in Fig.1. For a practical AMB-rotor system, more complex factors should be considered. It will take some time form the filter outputting signal to the rotor response turning into or at least closing to the steady state, which is called the transient time. So, the FIR filter is required to have the equal long memory time to match it. The time of impulse response decides the FIR filter’s memory which determined by the number of filter weights. The requirement of a long memory will significantly increase the computational complexity. Considering that the transient time is 0.1 s and the control sampling frequency is 10 kHz, 1000 weights will be required in the FIR filter. It is too difficult to realize the 4-DOF control algorithm with such complex computation. To deal with the requirement of a long impulse response, Fast Block LMS (FBLMS) algorithm is adopted to efficiently implement the computation of linear convolution and linear correlation at a computational cost far less than that of the conventional LMS algorithm of time domain. Additional, the FBLMS can adjust the convergence rate of the each individual frequency component of the signal. Next we will turn to the issue of how to suppress the vibration by applying the FBLMS algorithm.

2.1 FBLMS Algorithm Process

From digital signal-processing theory[13,18], we know that the overlap-save method provides an efficient procedure for computation of linear convolution and linear correlation by using the fast Fourier transform (FFT). Also, although the filter can be implemented with any amount of overlap, the use of 50 percent overlap is the most efficient. Hence, we focus our attention on the overlap-save method with 50 percent overlap, in which the block size equals to the number of filter weights. Fig. 3 shows a signal-flow graph representation of the fast block LMS (FBLMS) algorithm. This algorithm represents a precise frequency-domain implementation of the block LMS algorithm in the time domain.

Considering the FIR filter with *N* tap weights $W(k)$ in the time domain, according to the overlap-save method, the *N* tap weights of the filter are padded with an equal number of zeros, and a 2*N*-point FFT is used for the computation.

$$W_F^T(k) = FFT[W^T(k), \underbrace{0 \quad ... \quad 0}_{N}] \tag{25}$$

where $W_F(k)$,which is $2N$ -by-1 vector, denotes the frequency-domain weight vector and is the FFT coefficients of the zero-padded, tap-weight vector $W(k)$. The subscript $_F$ denotes the term in the frequency domain. $FFT[\ ]$ denotes fast Fourier transformation. Note that the frequency-domain weight vector $W_F(k)$ is twice as long as the time-domain weight vector $W(k)$.

The reference input signal sequence $x(n)$ is sectioned into *N*-point blocks. The *k*-th block is $X(k) = [x(kN), ..., x(kN + N - 1)]$. Let

$$X_F(k) = diag\{FFT[\underbrace{x(kN - N), ..., x(kN - 1)}_{(k-1)\text{th block}}, \underbrace{x(kN), ..., x(kN + N - 1)}_{k\text{th block}}]\} \tag{26}$$

denote a 2*N*-by-2*N* diagonal matrix obtained by Fourier transforming two successive blocks of the reference input signal. Hence, applying the overlap-save method to the linear convolution of $X(k)$ block and $W(k)$, yields the *N*-by-1 vector

$$OUT(k) = [out(kN), out(kN+1), ..., out(kN + N - 1)]^T = \text{last } N \text{ elements of } FFT^{-1}[X_F(k) W_F(k)] \tag{27}$$

where $FFT^{-1}[\ ]$ denotes inverse fast Fourier transformation. Only the last *N* elements in Eq. (27) are retained，due to the first *N* elements correspond to a circular convolution. Likewise, the control error signal sequence $y_{error}(n)$ is also sectioned into *N*-point blocks $Y_{error}(k) = [y_{error}(kN), ..., y_{error}(kN + N - 1)]$. Noting that the first *N* elements are discarded form output described in Eq. 27), we may transform the control error signal vector into the frequency domain as follows:

$$Y_{error\,F}(k) = FFT[\underbrace{0, ..., 0}_{N}, \underbrace{y_{error}(kN), ..., y_{error}(kN + N - 1)}_{k\text{th control error block}}]^T \tag{28}$$

Next, to calculate the *N*-by-1 gradient vector, the overlap-save method can be applied to the linear correlation of $X(k)$ and $Y_{error}(k)$ as follows

$$\nabla(k) = \text{ first } N \text{ elements of } \{-2FFT^{-1}[X_F^*(k) Y_{error\,F}(k)]\} \tag{29}$$

where * is the symbol for conjugate.

So, the frequency-domain weight vector is updated as.

$$W_F(k+1) = W_F(k) + \frac{1}{2}\mu FFT \begin{bmatrix} \nabla(k) \\ 0 \\ ... \\ 0 \end{bmatrix} \left.\begin{matrix} \\ \\ \\ \end{matrix}\right\} \ N \ zeros \tag{30}$$

where μ is the step-size parameter.

The procedure above is the algorithm process of the FBLMS. Finally, let's consider the frequency range for vibration suppressing which is dependent on the sampling frequency and the block size. if the sampling frequency is 10 kHz and the block size is defined as $N = 1024$, the frequency range of vibration suppressing will be from 10 Hz to 5 kHz.

In either the FBLMS algorithm or the conventional LMS algorithm, it is a important problem that the stability margin and the convergence rate of the different frequency component may be highly disparate in multi-frequency signal processing. The FBLMS algorithm is not only responsible for reducing the computational complexity, but also can make all frequency components converge at the same rate by assigning the different μ to each weight. Contrastively, the weights in the conventional LMS algorithm have not the intuitional relation with frequency.

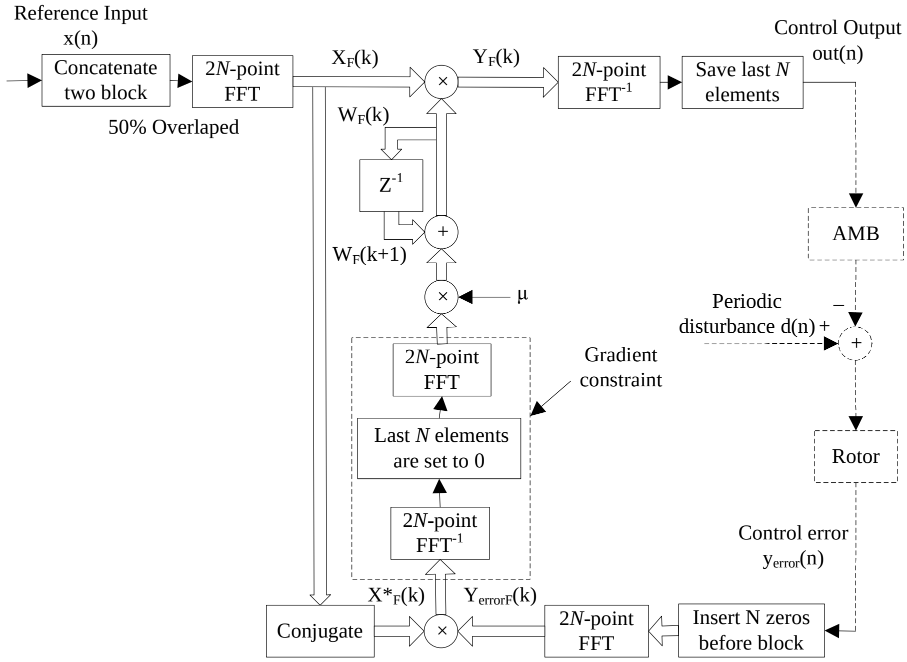

Fig.3 FBLMS algorithm applied in AMB

2.2 Choose of Reference Signal

According to Fig.1, the adaptive filter needs a reference input signal $x(n)$ which must have correlation with a disturbance $d(n)$. Here, the correlation between two signals means that two signals can be transformed each other by the certain unknown mapping relation. The adaptive filter will realize this mapping relation by adjusting the weights, so that the amplitude and phase of reference signal will match the disturbance vibration in each frequency component.

If the disturbance is measurable, the signal from disturbance measuring can directly be act as the reference signal. However, it is not easy to measure the disturbance in the most case. In this study, we choose the signal that composes of some sinusoids with the unit amplitude and zero phase, whose frequency is respectively equal to that of each disturbance component. In this way, the frequency distribution of disturbance must be known in advance and the objects of vibration suppressing are limited in periodic vibration.

2.3 Computational Complexity

The computational complexity of the FBLMS algorithm operating in the frequency domain is now compared with that of conventional LMS in the time domain. The comparison is based on a count of the total number of multiplications involved in each of these two implementations for generating the same block size N of control output $out(n)$. Although in an actual implementation, there are other factors to be considered (e.g. the consumption of additions and storage requirements), the use of multiplications provides a reasonable basis for comparing the computational complexity[13].

According to the references [13,18], for the FIR filter with N tap weights, the ratio of computational complexity for the FBLMS to the conventional LMS is

$$\frac{\text{FBLMS multiplications}}{\text{conventional LMS multiplications}}=\frac{10N\log_2 N+10N+16N}{2N^2}=\frac{5\log_2 N+13}{N} \tag{31}$$

When $N=32$, from Eq. (31), the computational complexities of two algorithms are similar. The more the tap weights of the filter are, the more efficient the FBLMS algorithm will be. For example, for $N=1024$, the FBLMS algorithm is roughly 15 times faster than the conventional LMS in computational terms.

3 Experimental results

3.1 AMB Rotor Test Rig

To confirm the effectiveness of the above algorithm, experiments were carried out on an AMB test rig with a vertical shaft shown in Fig. 4. The vertical shaft is supported by two radial AMBs. A coaxial brushless permanent magnetic motor is located between two radial AMBs. The axial support for the rotor is provided by a permanent magnetic bearing. The main parameters of the AMB-rotor system: the rotor weight including the flywheel $m=25.8kg$; the gap of back-up bearing $x=0.15mm$; the maximum rotating speed in experiment is 18000rpm (300Hz); The experiments were performed on d-SPACE DS 1103 with a sampling frequency of 10 kHz.

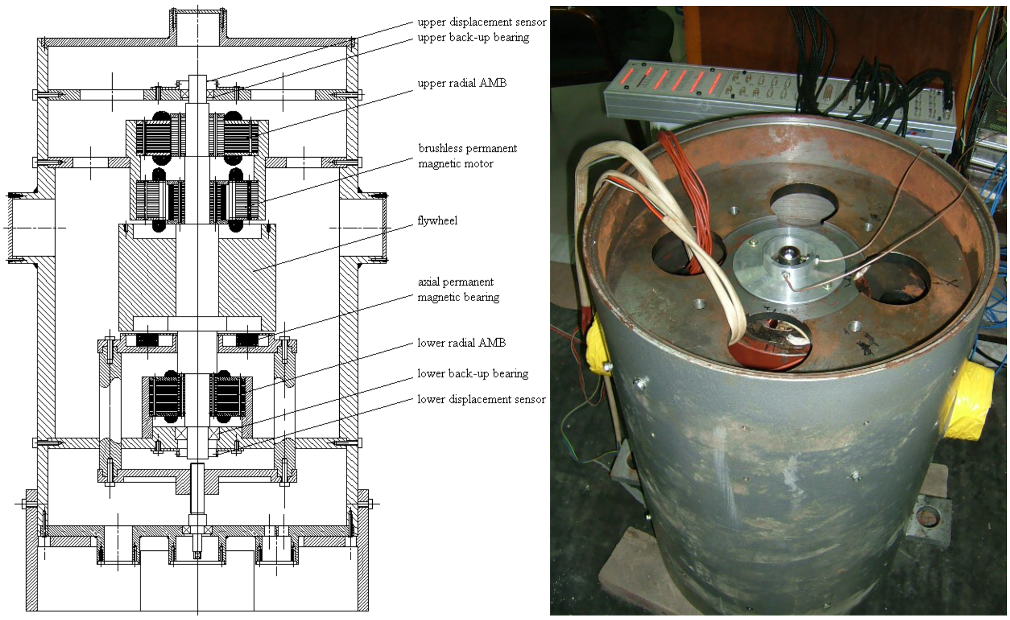

Fig.4 AMB test rig with vertical shaft

Firstly, the magnitude-frequency characteristic of the AMB-rotor system is measured as shown in Fig. 5. It is obviously that there are two vibration peaks approximately located in 14Hz and 25Hz within the range from 0 Hz to 200 Hz. Because the rotor is rigid, the frequencies of two peaks should be the first two rigid body critical frequencies of the rotor supported on the active magnetic bearings. Otherwise, above 100Hz, the values of the magnitude-frequency characteristic closes to zero. It means that the disturbance above 100 Hz would hardly excite the great vibration magnitude, unless the disturbance has a high energy level above 100 Hz.

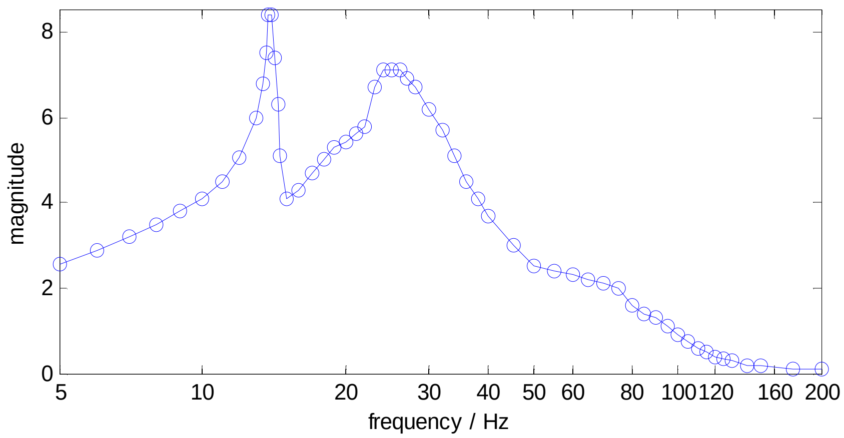

Fig.5 The magnitude-frequency characteristic of the AMB rotor system

3.2 Reciprocating Test for Simulating Disturbance

While the rotor is not rotating, a multi-frequency reciprocating vibration of rotor is excited by a simulating disturbance signal which is injected into the amplifier's input in the channel of the X-direction of the upper radial AMB. The disturbance signal consists of six sinusoidal components with same amplitude and different phase, which are 14 Hz, 25 Hz, 50 Hz, 75 Hz, 100 Hz, 125 Hz, respectively. Likewise, we choose the same six frequency components with the unit amplitude and zero phase as the reference input signal. In this experiment, the block size of FBLMS algorithm is chosen as $2N = 2048$. So the frequency range of vibration suppressing will be from 10 Hz to 5 kHz.

Fig. 6 shows the displacement sensor signal of the X-direction of the upper radial AMB in the time domain and its power spectrum distribution in the frequency domain without vibration suppressing. It is note that the displacement signal fluctuates in the time domain and there are six peaks in power spectrum which exactly correspond with the six disturbance components' frequency. Although the amplitudes of six frequency components in disturbance exciting are equal, their responses are different whose magnitudes are consistent with the test results shown in Fig. 5. The peak in 125 Hz can hardly be distinguished in the system noise.

With multi-frequency vibration suppressing, as shown in Fig 7, it is clear that the displacement signal fluctuation is significantly diminished. The original six peaks of disturbance in power spectrum are completely vanished in noise, which proves that multi-frequency vibration suppressing of the rotor is very effective.

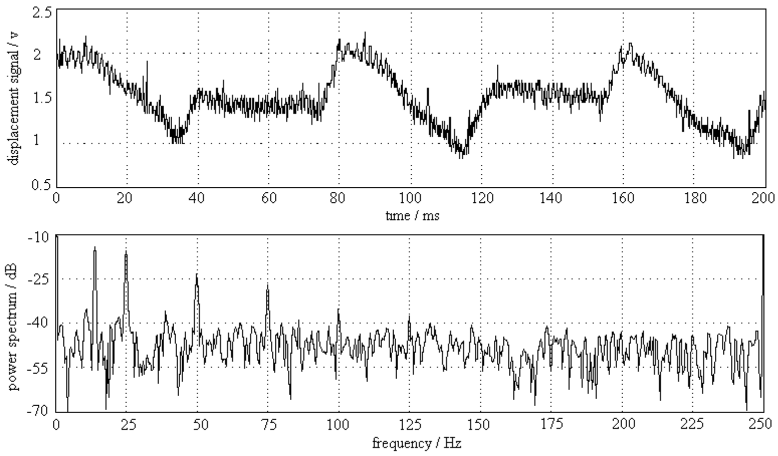

Fig.6 Displacement signal and power spectrum distribution without vibration suppressing

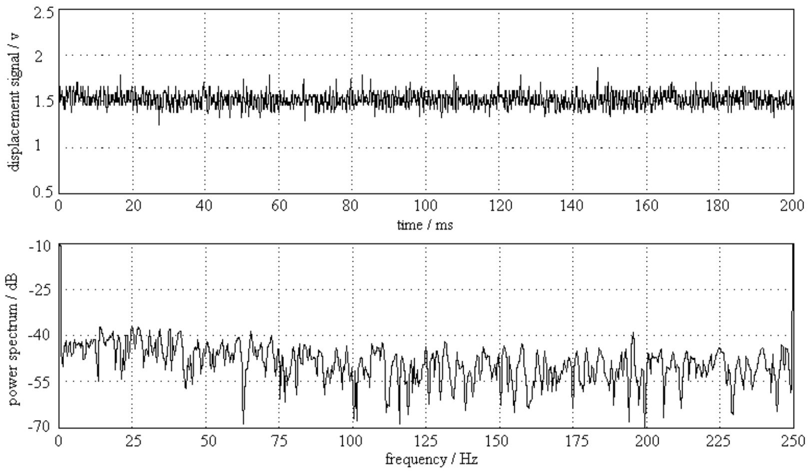

Fig.7 Displacement signal and power spectrum distribution with vibration suppressing

In experiments, the process that six peaks are gradually collapsed one by one can be clearly observed. The convergence rates of different frequency peaks are different, moreover, are possibly divergent in some frequency. Fortunately, the convergence properties of each frequency can be adjusted conveniently by assigning an individual μ_i to the corresponding weight in the FBLMS.

3.3 Rotating Test

In the AMB test rig, the rotor is driven by a coaxial brushless permanent magnetic motor with 4 poles. It is found that the permanent magnetic motor in normal operation would generate a radial disturbance force whose frequency is multiple of the rotating frequency. Fig. 8(a) shows the vibration power spectrum of X-direction in the upper AMB at a given steady rotational speed of 1500 rpm (25 Hz). Besides the rotor unbalance vibration of 25 Hz, it can be observed that many high harmonic frequencies exist in the vibration. Among the high harmonic frequencies, the second and the fourth harmonic frequencies are extremely outstanding and the third one is comparatively a little weak. Other higher harmonic frequencies are inconspicuous in Fig. 8(a). As a result, the rotor rotating orbit is not in a circle as shown in Fig. 8(b) because of the many high harmonic frequencies existing.

In this test, to suffice for the computational complexity of 4 DOF, the block size of the

FBLMS algorithm is reduce to $2N = 1024$. So, the frequency range of vibration suppressing will be from 20 Hz to 5 kHz.

In the FBLMS algorithm, each frequency component of disturbance vibration can be addressed respectively by reconfiguring the frequency components of the reference input signal. In this test, the reference input signal is configured to contain 50 Hz, 75 Hz, 100 Hz and does not include 25 Hz. When the vibration suppressing is activated, the vibration power spectrum of X-direction in the upper AMB at a given steady rotational speed of 1500 rpm (25 Hz) is shown in Fig. 9(a). It is shown that the vibrations of the high harmonic frequencies are suppressed and the fundamental harmonic is remained. As a result, the rotor orbit becomes an ellipse as shown in Fig. 9(b). Because of the different of the rotor supporting stiffness in each DOF, the rotor orbit is not a circle but an ellipse.

Then, the frequency of 25 Hz is added to the reference input signal. The experiment result with all harmonics suppressing is shown in Fig. 10(a). The peak of the fundamental harmonic at 25 Hz also is vanished and the rotor orbit visibly converges toward its center in Fig. 10(b).

4 Conclusion

In this study, the multi-frequency periodic vibration suppressing method based on the FBLMS algorithm is adopted for the AMB-rotor system at a computational cost far less than that of the conventional LMS algorithm. The unique feature of the FBLMS algorithm is characterized by no influence on the computational complexity, regardless of the number of the disturbance frequency components within the range of sampling frequency. Moreover, the weights in the FBLMS algorithm have the intuitional relation with frequency. As a result, each harmonic components of the vibration can be addressed respectively or together. The experimental results for the reciprocating simulating disturbance test and the rotating harmonic vibration test show that the proposed adaptive structure with the FBLMS algorithm can achieves the good effectiveness for suppressing the multi-frequency periodic vibration.

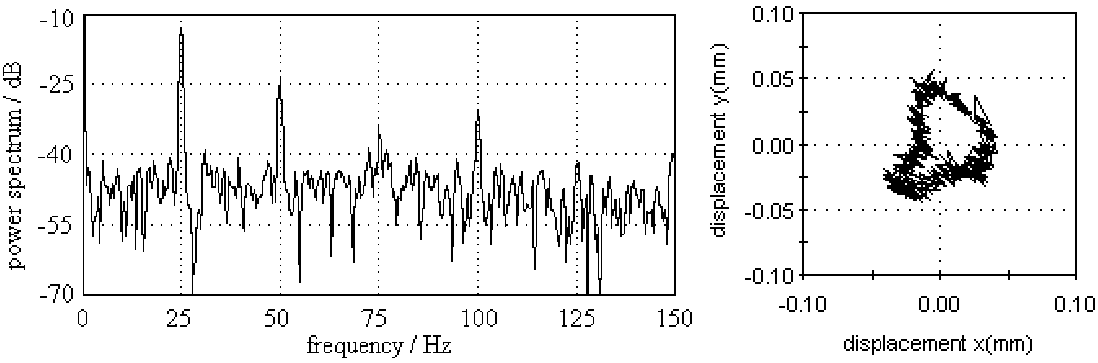

(a) (b)

Fig.8 power spectrum distribution and orbit of rotor vibration without vibration suppressing

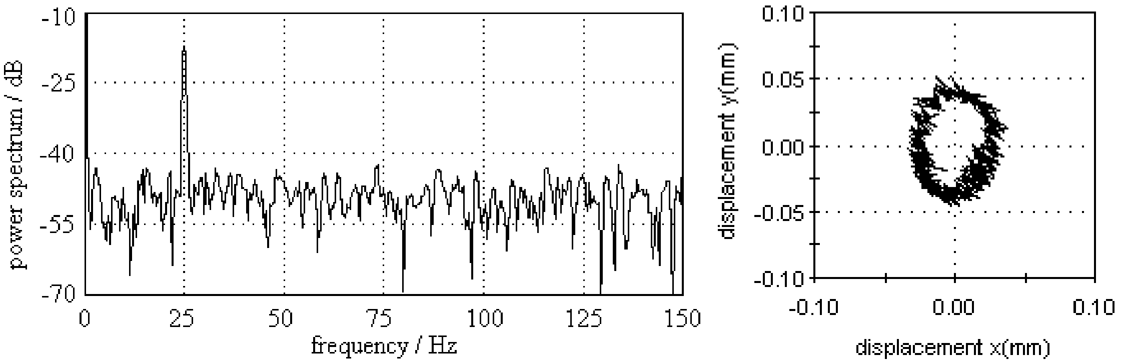

Fig.9 power spectrum distribution and orbit of rotor vibration with high harmonics suppressing

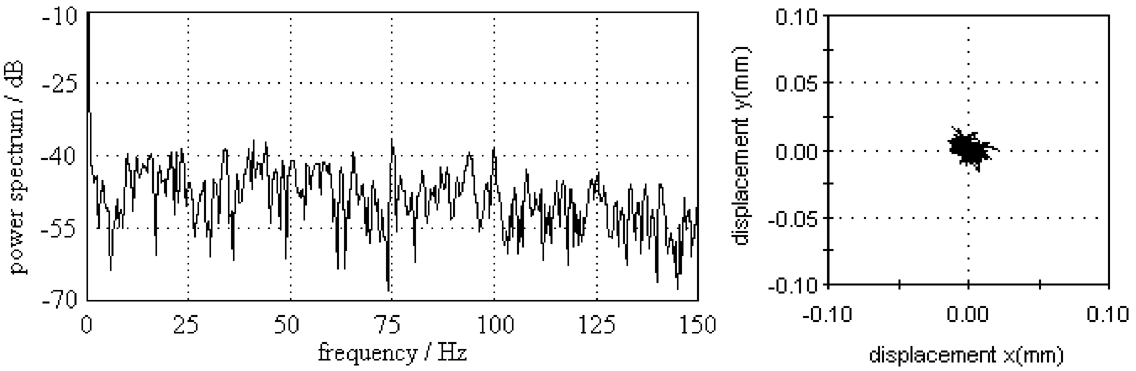

Fig.10 power spectrum distribution and orbit of rotor vibration with all harmonics suppressing

ACKNOWLEDGEMENT

The research was supported by the National High Technology Research and Development Program of China (2006AA05Z201) and the National Natural Science Foundation of China (10772160).

Reference

[1] J. Shi, R.Zmood, and L. J. Qin: *The direct method for adaptive feed-forward vibration control of magnetic bearing systems*. Proceedings of the 7th International Conference on Control, Automation, Robotics and Vision, Singapore, (2002), p. 675-680.

[2] L. Tang and Y. Chen: *Research on adaptive filter control of imbalance vibration*. Journal of Astronautics, 28(6)(2007), p.1569-1574 (in Chinese).

[3] G. Hector and S. M. Pablo: *Unbalance compensation for active magnetic bearing using ILC*. Proceedings of IEEE International Conference on Control Applications, Mexico, (2001), p.58-63

[4] S. Beale, B. Shafai: *Adaptive forced balancing for magnetic bearings control systems*. Proceedings of the 31st Conference on Decision and Control, (1992), p. 3535-3539.

[5] E. Vahedforough, B. Shafai, S. Beal: *Estimation and rejection of unknown sinusoidal disturbances using a generalized adaptive forced balancing method*. Proceedings of the 2007 American Control Conference, (2007), p.3529-3534.

[6] K. Nonami, Q. Fan: *Unbalance vibration control of magnetic bearing systems using adaptive algorithm with disturbance frequency estimation.* Proceedings of the 6th International Symposium on Magnetic Bearings. MIT, Cambridge, Masscahusetts, USA, (1998), p.663-672.

[7] J. Setiawan and R. Mukherjee: *Adaptive compensation of sensor runout and mass unbalance in MB system*. Proceedings of IEEE/ASME International Conference on Advanced Intelligent Mechatronics, (1999),

p.800-805.

[8] K. Nonami, Z. Liu: *Adaptive unbalance vibration control of MB system using frequency estimation for multiple periodic disturbances with noise*. Proceedings of IEEE International Conference on Control Application, (1999), p. 576-581.

[9] Sahinkaya M N. Cole M O T and Burrows C R. *On the use of schroeder phased harmonic sequences in multi-frequency vibration control of flexible rotor/magnetic bearing systems.* Proceedings of the 8th International Symposium on Magnetic Bearings, Mito, Japan, August (2002), p.217-222.

[10] Z. Liu. and K. Nonami: *Adaptive unbalanced vibration control of magnetic bearing system with rotational synchronizing and asynchronizing harmonic disturbance.* JSME International Journal, Series C, 45(1), (2002),p.142-149.

[11] Cole M.O.T.: *Robust control of multiple discrete frequency vibration components in rotor magnetic bearing systems*. JSME International Journal, Series C, 46(3), (2003), p.891-899.

[12] S. Hong and R. Langari: *Robust fuzzy control of a magnetic bearing system subject to Harmonic disturbances.* IEEE Transactions on Control Systems Technology, 8(2), (2000), p.366-370

[13] Simon Haykin: *Adaptive filter theory(fourth edition).* (Upper Saddle River, NJ, Prentice Hall, 2002).

[14] Robert G B: *Introduction to random signal analysis and Kalman filtering*. (John Wiley &Sons, Inc., USA, 1983).

[15] K Sam Shanmugan and Arthur M Breipohl: *Random signals: detection, estimation and data analysis.* (John Wiley &Sons, Inc., USA. 1988)

[16] B. Widrow and S. Stearns: *adaptive signal processing*. (Upper Saddle River, NJ: Pearson/Prentice Hall, USA, 2008).

[17] C. F. N. Cowan and P. M. Grant: *adaptive filters.* (Prentice-hall Inc, USA.1985)

[18] S R D. Paulo: *Adaptive filtering; algorithms and partial implementation (second edition)* (in Chinese). (Publish House of Electronics Industry, China. 2004).